Measurement of e^+e^- Annihilation at Rest into Four γ Rays

Shunji Adachi, Masami Chiba, Tachishige Hirose, Shojiro Nagayama, Yuki Nakamitsu, Toshiyuki Sato, and Tadashi Yamada

Department of Physics, Tokyo Metropolitan University, 2-1-1 Fukazawa, Setagaya-ku, Tokyo 158, Japan

(Received 27 July 1990)

We have measured for the first time the decay rate for $e^+e^- \rightarrow 4\gamma$ from the e^+e^- singlet state at rest, by using a multi-γ-ray spectrometer. The branching ratio $R = \lambda_S^{4\gamma}/\lambda_S^{2\gamma}$, where $\lambda_S^{4\gamma}$ and $\lambda_S^{2\gamma}$ are the 4γ and 2γ decay rates, respectively, was measured to be $R = [1.30 \pm 0.26(\text{stat}) \pm 0.16(\text{syst})] \times 10^{-6}$, consistent with the lowest-order QED calculation.

PACS numbers: 12.20.Fv, 13.10.+q

A study of 4γ annihilations from e^+e^- states at rest provides an important means for checking quantum electrodynamics (QED) with multiple vertices, although it is difficult to measure 4γ annihilations owing to the extremely small annihilation rate compared to 2γ annihilations. In 1974 Marko and Rich searched for the C-parity-forbidden 4γ decay from the e^+e^- triplet state and obtained a result consistent with C-parity conservation.[1] However, a deviation from the QED prediction for the 3γ decay rate was reported.[2] In the present paper we report the first results of $e^+e^- \rightarrow 4\gamma$ at rest, in terms of the branching ratio $R = \lambda_S^{4\gamma}/\lambda_S^{2\gamma}$, where $\lambda_S^{4\gamma}$ and $\lambda_S^{2\gamma}$ represent the annihilation rates into four and two γ rays, respectively. The lowest-order QED calculation for R has been made[3] and the latest result is given by Adachi as $(1.4796 \pm 0.0006) \times 10^{-6}$. Before the present investigation, a preparatory experiment was carried out by Watanabe[4] to study how to detect four γ rays efficiently, free of backgrounds. It was found that serious γ-ray backgrounds emerged both from Compton scattering in the NaI(Tl) scintillator and the target and from bremsstrahlung of the positron in the target.

Taking into account the knowledge thus obtained, we constructed a multi-γ-ray spectrometer by utilizing 32 NaI(Tl) scintillation counters, each located on a surface of an icosidodecahedron. Figure 1(a) shows the cross section of the spectrometer[5] containing eight modules. One module consists of an NaI(Tl) scintillator with lead collimator and a photomultiplier tube (PMT: Hamamatsu R1911, with a diameter of 3 in.). The size of the NaI(Tl) crystals in $76.2^{+0}_{-0.15}$ mm in diameter and $101.6^{+0.5}_{-1.0}$ mm in length. We carefully fabricated the windows of the NaI(Tl) scintillators to achieve efficient detection of low-energy γ rays, using 0.5-mm-thick pure aluminum plates, 4-mm-thick rubber for cushions, and light-reflection papers of thickness 0.22 mm instead of the MgO powder normally used. The front face of an NaI(Tl) crystal is located at a distance of 261.6 ± 0.6 mm from the center of the spectrometer, covering a solid angle of $(0.521 \pm 0.005)\%$ of 4π sr. We designed the lead collimators so that γ rays arising from Compton scattering on the surface of an NaI(Tl) scintillator cannot enter another NaI(Tl) scintillator. In our detector, a γ ray scattered on the surface of an NaI(Tl) scintillator must penetrate at least 30 mm of lead to enter another crystal, except for the back-to-back configuration. Hence Compton-scattering γ rays of energy of 300 keV can be suppressed by a factor of 10^{-6}. The typical energy resolution of the NaI(Tl) scintillator is $\sigma/E = (19.9/\sqrt{E} + 2.34)\%$ (E in keV). Signals from 32 PMTs are independently fed to discriminators, CAMAC scalers, analog-to-digital converters, and time-to-digital converters.

As shown in Fig. 1(b) the positron source, 0.26-MBq ^{68}Ge, with diameter of 4 mm and thickness of 0.5 mm, is placed between two plastic scintillators (NE102A) with

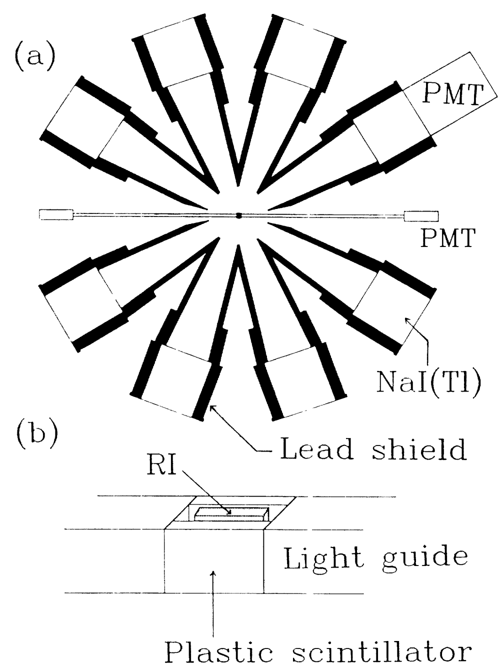

FIG. 1. (a) Cross section of the multi-γ-ray spectrometer. (b) Bird's-eye view around the trigger scintillator. The shading shows the radio isotope which is located between two plastic scintillators.

dimensions of $1\times10\times15$ mm^3. The ^{68}Ge decays into ^{68}Ga only through electron capture, with a half-life of 288 days. Then ^{68}Ga decays into the ground state of ^{68}Zn with a branching fraction of 89% through β^+ decay whose maximum kinetic energy is 1889 keV. The excited state of ^{68}Zn is also populated in this β^+ decay, with the fraction 1.3%, emitting a transition γ ray of 1077 keV. The positrons lose their energy and annihilate with electrons in the plastic scintillators. The light produced in the plastic scintillator (trigger scintillator) is guided by two acrylic light guides with dimensions of $4\times10\times320$ mm^3 to two PMTs (Hamamatsu R647) on either side, as shown in Fig. 1. We use this counter system as a trigger counter in order to know the number of e^+ and the emitted time of the e^+. The performance of the trigger scintillator is investigated by a Monte Carlo simulation which is based on EGS 4 (Ref. 6), with a kinetic-energy cutoff of 10 keV for electrons and photons. This simulation takes account of the energy spectrum of e^+ from ^{68}Ga and the complete geometry of the target region, containing the isotope, the trigger scintillators, light guides, glue, aluminum-foil reflectors, and light-shielding tapes. This simulation program clarifies that at the target 84.8% of all e^+ from ^{68}Ga lose their full energy and thus annihilate. The fraction of annihilations was estimated to be 79.1% when the trigger scintillator was set at a certain threshold level of discrimination which was determined from the correlation between the threshold level and the counting rate: This correlation is well reproduced by the Monte Carlo simulation. The fraction of in-flight annihilation was found to be 2.8%, which is consistent with the result (3%) of Ref. 7. The annihilation takes place predominantly through spin-singlet states, but triplet states remain with a ratio of $1\,^3S_1/1\,^1S_0=2.32/372$,[8] giving rise to backgrounds mentioned later.

The trigger condition for data taking is provided by the coincidence of the trigger counter and any four of the NaI(Tl) scintillators, and the veto from any two counters located back to back. The large amount of 2γ annihilation events is effectively suppressed by the veto. For this trigger condition, we collected 80474 events for 1.2×10^{12} e^+ counted by the trigger counter.

Since the branching ratio for $e^+e^-\to4\gamma$ is extremely small, it is essential to estimate accurately the possible backgrounds. Using the Monte Carlo program, which contains an event generator and detector simulator, we obtain in Table I the relative contributions of 29 different background processes. For the generation of the events $e^+e^-\to3\gamma,4\gamma$, we used a series of programs, i.e., GRAND,[9] REDUCE,[10] and BASES/SPRING.[11] The EGS 4 code is utilized for electromagnetic processes in the detector simulation which includes the complete geometry in the trigger region mentioned above, air, the lead collimators, and the NaI(Tl) scintillators. To check how well our Monte Carlo program reproduces experimental data, we attempted to compare the Monte Carlo events

TABLE I. Trigger ratio of backgrounds compared to the 4γ annihilation events (relative yield 1.0) with a 0.26-MBq ^{68}Ge source. Accidental coincidence (simultaneous occurrence) is represented with $\times$ ($+$). ($2\gamma-$Compton) means that one of 2γ rays in 2γ annihilation is scattered in the trigger region. $\gamma(\gamma)$ stands for 2γ annihilation with one γ missing, and $\gamma\gamma(\gamma)$ and $\gamma(\gamma\gamma)$, 3γ annihilations with one and two γ missing, respectively. γ_B (γ_T) corresponds to bremsstrahlung (transition γ ray). e^+ denotes a positron through the trigger counter, and e^-, an electron struck out of the trigger region by a positron or a γ ray.

No.	Backgrounds	Relative yield
1	$(2\gamma-\text{Compton})\times(2\gamma-\text{Compton})$	37.8
2	$3\gamma\times\gamma(\gamma)$	7.0
3	$(2\gamma-\text{Compton})\times\gamma\gamma(\gamma)$	5.3
4	$3\gamma\times$noise	1.7
5	$[e^-+(2\gamma-\text{Compton})]\times\gamma(\gamma)$	8.5×10^{-1}
6	$\gamma\gamma(\gamma)\times\gamma\gamma(\gamma)$	7.3×10^{-1}
7	$3\gamma\times\gamma(\gamma\gamma)$	4.8×10^{-1}
8	$[e^-+(2\gamma-\text{Compton})]\times e^+$	2.7×10^{-1}
9	$e^+\times3\gamma$	2.2×10^{-1}
10	$(2\gamma-\text{Compton})\times2\gamma_T$	8.0×10^{-2}
11	$[\gamma\gamma(\gamma)+\gamma_B]\times$noise	3.8×10^{-2}
12	$\gamma\gamma(\gamma)\times\gamma(\gamma)\times\gamma(\gamma)$	1.3×10^{-2}
13	$(2\gamma-\text{Compton})\times\gamma(\gamma)\times\gamma(\gamma\gamma)$	6.4×10^{-3}
14	$[e^-+(2\gamma-\text{Compton})]\times\gamma(\gamma\gamma)$	2.9×10^{-3}
15	$e^+\times e^+\times[\gamma(\gamma)+\gamma_B]$	2.9×10^{-6}
16	$(e^++\gamma_B)\times e^+\times\gamma(\gamma\gamma)$	2.5×10^{-7}
17	$e^+\times e^+\times\gamma(\gamma)\times\gamma(\gamma)$	2.2×10^{-7}
18	$(e^++\gamma_B)\times e^+\times e^+$	1.1×10^{-7}
19	$e^+\times e^+\times e^+\times\gamma(\gamma)$	7.2×10^{-9}
20	$(2\gamma-\text{Compton})\times\gamma(\gamma)\times\gamma(\gamma)$	2.5×10^{-9}
21	$e^+\times e^+\times e^+\times\gamma(\gamma\gamma)$	2.5×10^{-10}
22	$e^+\times e^+\times e^+\times e^+$	2.3×10^{-10}
23	$(3\gamma+\gamma_B)$	70.1
24	$(3\gamma+\gamma_T)$	35.0
25	$[(2\gamma-\text{Compton})+2\gamma_B]$	10.8
26	$[\gamma\gamma(\gamma)+2\gamma_B]$	1.4
27	$[e^-+(2\gamma-\text{Compton})+\gamma_B]$	9.0×10^{-1}
28	$[\gamma\gamma(\gamma)+\gamma_B+\gamma_T]$	8.1×10^{-1}
29	$[e^-+(2\gamma-\text{Compton})+\gamma_T]$	4.0×10^{-1}

with data for 2γ annihilations. It was found that the detection efficiency of 2γ events was precisely reproduced to an accuracy of 0.8%.

Backgrounds are classified into two categories, namely, accidental coincidence and simultaneous occurrence. The accidental coincidence is attributed to the fact that two different events occurring within the coincidence width of 10 nsec cannot be discriminated. Another type of background, i.e., the simultaneous occurrence, is observed if the annihilations take place in association with the bremsstrahlung γ ray or the transition γ ray. We give our estimated relative yields of backgrounds in Table I, in which 22 processes for accidental coincidence and 7 processes for simultaneous occurrence are taken into account. The third column in Table I shows the rel-

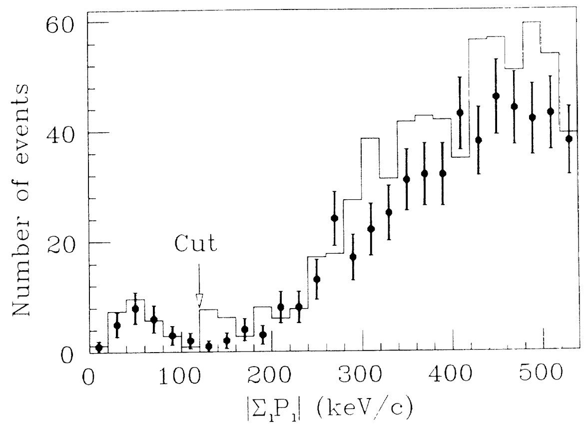

FIG. 2. Distribution of the momentum balance. Points are the experimental data, and the histogram is the Monte Carlo results, which is normalized by the number of e^+.

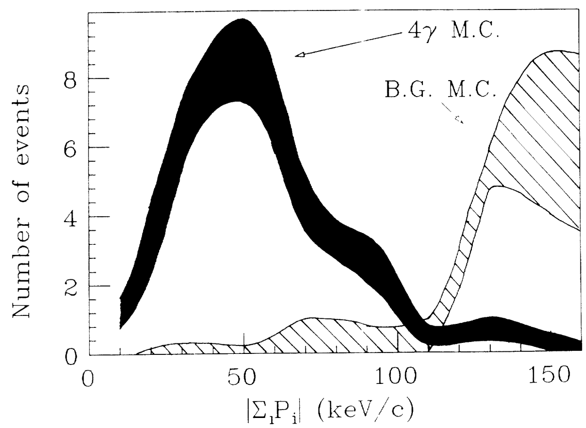

FIG. 3. The Monte Carlo results of the overlap region. The shaded and hatched regions represent the error of the Monte Carlo calculation.

ative yield of backgrounds versus genuine 4γ events.

Candidates for 4γ events are selected by the following criteria: (1) time difference between the e^+ emitted time and the time when a γ ray hits the NaI(Tl) scintillator being about 10 nsec, (2) the sum-energy cut for four γ rays (900 keV $\leq \sum_{i=1}^{4} E_i \leq$ 1100 keV) being effective for all kinds of backgrounds, and (3) the rejection of coplanar events due to $e^+e^- \rightarrow 3\gamma$. After these selection processes (1)-(3), the original number of events 80474 decreases to 17371, 4302, and 1351, respectively. Finally, we examine for the 1351 events the momentum balance of four γ rays (Fig. 2) and obtain 26 events after applying the condition (4) $|\sum_{i=1}^{4} \mathbf{P}_i| \leq 120$ keV/c, where $\mathbf{P}_i$ is the momentum vector of the ith γ ray emitted. The momentum-balance resolution is determined to be 26 keV/c from the peak corresponding to 4γ events as seen in Fig. 2. The contamination for 26 events is estimated to be 0.74 event in which 0.63 event arises from the accidental coincidence and 0.11 event from the simultaneous occurrence. Figure 3 shows the overlap region between 4γ and the background studied by the Monte Carlo simulation. We found 24% for the fraction (F) of genuine Monte Carlo 4γ events surviving the selection criteria mentioned above.

Ambiguities in the NaI(Tl) crystal size and the position of the NaI(Tl) result in an error of geometrical acceptance for 4γ (4.5%). The Monte Carlo simulation contains statistical errors for 4γ events (7.9%), background events (7.9%), and errors of detection efficiency (1.6%).

The branching ratio R is derived according to the following relation:

$$R = (N_{\rm obs} - N_{\rm back})/N_{e^+} R_{\rm trig} \epsilon F\,.$$

The various quantities used are defined as follows: $N_{\rm obs}$ is the number of the 4γ events observed (26); $N_{\rm back}$ is the expected number of background events (0.74); N_{e^+} is the number of positrons counted by the trigger scintillator (1.2×10^{12}); $R_{\rm trig}$ is the ratio of stopped e^+ in the trigger scintillator against the number counted by the trigger scintillator (0.84); ϵ is the detection efficiency of the NaI(Tl) scintillators for the 4γ annihilation (8.1

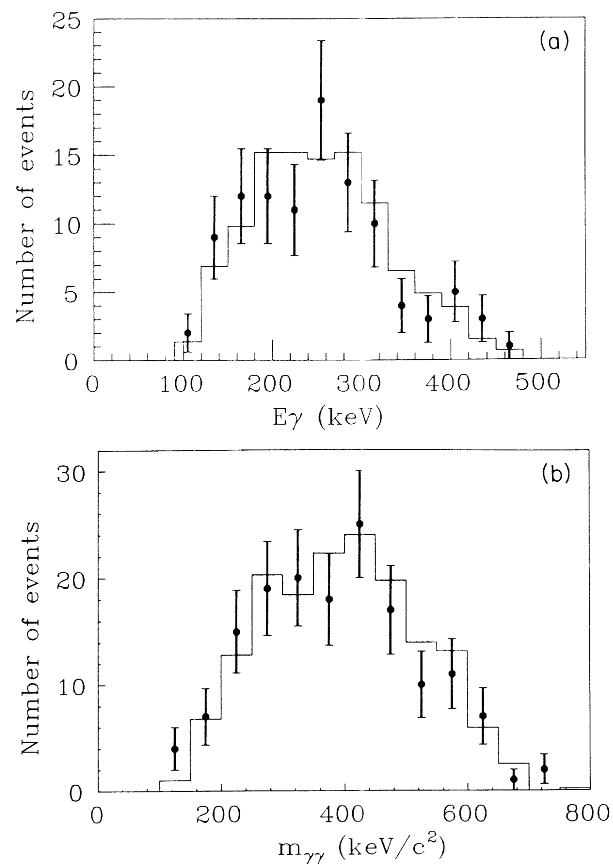

FIG. 4. (a) Energy distribution of 1γ and (b) invariant-mass distribution of 2γ for 4γ events. Points are the experimental data. Histogram shows the Monte Carlo data normalized by the number of e^+.

$\times 10^{-5}$); F is the fraction of 4γ events surviving the selection criteria (0.24). We obtained $R=[1.30 \pm 0.26(\text{stat}) \pm 0.16(\text{syst})] \times 10^{-6}$ which is consistent with the theoretical value within 1σ. For 26 4γ events, we plot the energy distribution of single-γ events in Fig. 4(a) and the invariant-mass distribution of 2γ events for all combinations in Fig. 4(b), together with the Monte Carlo calculation based on QED of order α^4.

We successfully measured the e^+e^- annihilation at rest into four γ rays, rejecting the heavy backgrounds. We verify that QED agrees well with data even at this low energy. We are still accumulating 4γ events by improving the intensity of the isotope by a factor of 4, and thus the statistical precision is expected to improve to around 0.1×10^{-6}.

We sincerely thank Dr. K. Endo and Y. Watanabe for their kind advice about making the ^{68}Ge source. We also thank Dr. S. Kitamura for the computational work. This work was partially supported by a grant in aid for scientific research from the Ministry of Education of Japan.

[1]K. Marko and A. Rich, Phys. Rev. Lett. **33**, 980 (1974).

[2]C. I. Westbrook *et al.*, Phys. Rev. A **40**, 5489 (1989).

[3]G. McCoyd, Ph.D. thesis, St. John's University, New York, 1965 (unpublished); A. Billoire, R. Lacaze, A. Morel, and H. Navelet, Phys. Lett. **78B**, 140 (1978); T. Muta and T. Niuya, Prog. Theor. Phys. **68**, 1735 (1982); G. S. Adkins and F. R. Brown, Phys. Rev. A **28**, 1164 (1983); G. P. Lepage *et al.*, Phys. Rev. A **28**, 3090 (1983); S. Adachi, Bachelor's thesis, Tokyo Metropolitan University, 1990 (unpublished).

[4]T. Watanabe, M.S. thesis, Tokyo Metropolitan University, 1987 (unpublished).

[5]S. Adachi *et al.* (to be published).

[6]W. R. Nelson, H. Hirayama, and D. W. O. Rogers, SLAC Report No. SLAC-Report-265, 1985 (unpublished).

[7]W. Heitler, *The Quantum Theory of Radiation* (Oxford Univ. Press, London, 1954), 3rd ed.

[8]A. Ore and J. L. Powell, Phys. Rev. **75**, 1696 (1949); S. DeBenedetti and R. T. Siegel, Phys. Rev. **94**, 955 (1954); J. K. Basson, Phys. Rev. **96**, 691 (1954); M. Bertolaccini *et al.*, Phys. Rev. **139**, A696 (1965); M. Bertolaccini *et al.*, Phys. Rev. Lett. **63**, 597 (1989).

[9]T. Kaneko, S. Kawabata, and Y. Shimizu, Comput. Phys. Commun. **43**, 279 (1987).

[10]A. C. Hearn, REDUCE user's manual ver. 3.3, July 1987, Rand Publication CP78 (Rev. 7/87).

[11]S. Kawabata, Comput. Phys. Commun. **41**, 127 (1986).

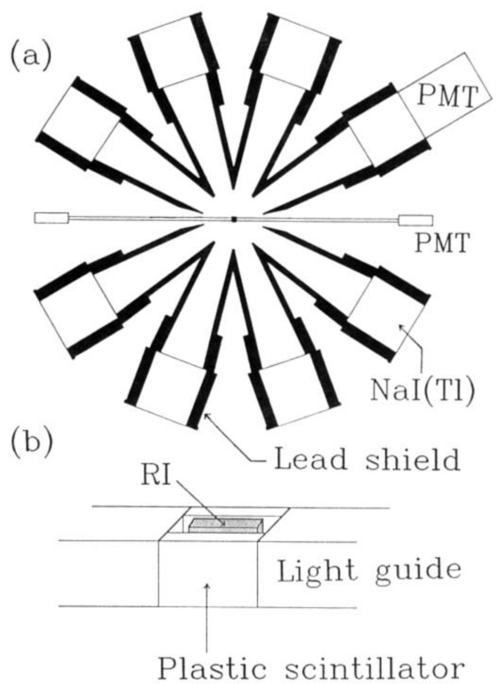

FIG. 1. (a) Cross section of the multi-γ-ray spectrometer. (b) Bird's-eye view around the trigger scintillator. The shading shows the radio isotope which is located between two plastic scintillators.